Long-term *ex ovo* culture of *Caenorhabditis elegans* embryos

Clover Ann Stubbert[1], Cherry Soe[2], Pavak Kirit Shah[1,2,3,*]

1. Molecular Biology Institute. University of California, Los Angeles. University of California, Los Angeles. Los Angeles, CA 90095 USA
2. Department of Molecular, Cell and Developmental Biology. University of California, Los Angeles. Los Angeles, CA 90095 USA
3. Institute for Quantitative and Computational Biosciences. University of California, Los Angeles. Los Angeles, CA 90095 USA

*Corresponding author: Department of Molecular, Cell and Developmental Biology, University of California Los Angeles, 610 Charles E Young Dr S, Los Angeles, CA 90095, USA. Email: pavak@ucla.edu

Abstract

While the genetic tractability, transparency and invariant development of the *Caenorhabditis elegans* embryo have led to its broad adoption as a model system for the study of cell and developmental biology, its impermeable eggshell has complicated the use of small-molecule reagents during embryogenesis. Existing genetic approaches for rendering the embryo permeable to acute small molecule treatment have increased the accessibility of early embryogenesis to pharmacological manipulation but compromise long-term viability, preventing their use in studies of later developmental processes or post-exposure physiology. Here, we describe the use of an optimized enzymatic eggshell digestion protocol coupled with a minimal, serum-free culture media that supports the survival and normal development of *ex ovo* embryos through larval maturation and adulthood. We show that this approach renders embryos permeable to a wide range of small molecules, enabling precise temporal manipulation of developmental processes previously inaccessible through conventional genetic methods. We demonstrate the utility of this technique through the application of small molecule fluorescent dyes, the pharmacological modulation of cytoskeletal components including microtubules and actin, as well as the minus-end-directed microtubule motor protein dynein, highlighting applications for study of cell division, morphogenesis, and neuronal cell biology, especially in later stages of embryogenesis. This approach expands the experimental toolkit available for labeling and manipulating developmental processes in *C. elegans*.

Introduction

The nematode *Caenorhabditis elegans* is a powerful model system for the study of genetics, development, and cell biology owing to its genetic tractability, transparency across life stages, and invariant development. In contrast to the amenability of the *C. elegans* embryo to live

imaging[1,2], advances in the perturbation of developmental processes have been primarily limited to genetic[3,4] and optical approaches[5–8] by the impermeability of its eggshell, consisting of multiple proteoglycan and chitin layers[9]. This renders *C. elegans* embryos impermeable to most small molecules.

A genetic screen previously identified multiple genes (*perm-1, perm-2*) required for the eggshell permeability barrier[10]. Knock-down of these genes by RNAi causes the generation of embryos whose eggshells are permeable to small molecules, which has enabled a wide range of pharmacological manipulations of the early embryo[11–15]. This approach has some drawbacks, as it results in small brood sizes and compromised viability with embryos typically arresting around gastrulation[10,16], making it unusable for the labeling and manipulation of later developmental stages. Physical methods of permeabilizing the eggshell (laser ablation[17,18], acute coverslip pressure[19,20], and microinjection[21]) also have been used to introduce small molecules into *C. elegans* embryos but are limited in throughput and introduce sources of variability such as the magnitude of applied pressure and the targeting of the laser microbeam. Shelton's media has been used in combination with each of these permeabilization strategies to increase the viability of permeabilized embryos[22–24].

Cell culture systems are inherently more compatible with small molecule treatments and the *in vitro* culture of *C. elegans* embryonic cells has been extensively demonstrated in the literature. Generally, these approaches involve the recovery of embryos by dissociating gravid adults using alkaline hypochlorite followed by eggshell removal via digestion by chitinase. The exposed embryos are then released from the peri-embryonic layer and disaggregated by shear stress (such as by aspiration through a fine needle) to then be cultured in a range of media conditions that can support the development of early blastomeres[25] or the growth and survival of differentiated neurons and muscle cells[26].

We reasoned that an approach based on these cell culture techniques, especially given the adoption of Shelton's media in combination with permeabilization strategies, may be able to support the long-term culture of fully eggshell-removed, yet intact embryos. Indeed we have found that optimized eggshell digestion protocols, when combined with a simplified serum-free culture media, supports the survival and growth of embryos through larval maturation, producing healthy individuals that are able to be transferred to standard culture plates and raised to fertile adulthood. Since others have previously shown that chitinase digestion is sufficient to render embryos permeable to fluorescent dyes[27], we tested whether these cultured embryos are compatible with manipulation by many common small molecules (eg. dyes, toxins, and selective inhibitors) at developmental stages that are not accessible by *perm-1* and *perm-2* RNAi. We demonstrate that these treatments can be used to manipulate a wide range of biological processes and structures within the *C. elegans* embryo including the microtubule and actin cytoskeleton and the activity of the minus end-directed microtubule motor protein dynein. This

work provides a scalable approach that expands the toolkit available for the labeling and manipulation of the *C. elegans* embryo for studies of development and cell biology.

Results

Ex ovo culture of *C. elegans* embryos

Genetic perturbations that render the eggshell permeable to small molecules also reduce viability[10], making these approaches incompatible with studies of developmental processes that occur after gastrulation such as tissue morphogenesis and neuronal development. We hypothesized that media optimized for nematode embryonic cell culture may support embryo viability in the absence of the eggshell permeability barrier. We use a simplified version of a culture media originally developed for maintaining *C. elegans* neuronal and muscle cells in culture[26], omitting the serum the original protocol used so as not to provide the intact embryo with exogenous growth factors. This minimal media is prepared from commercially available Leibovitz' L-15 media supplemented with 7.7 g sucrose / 500 mL and 1× penicillin and streptomycin (can be omitted for short-term culture).

To test the ability of this media to support embryo viability, we first prepared embryos for digestion by collecting worms and embryos from a 60 mm nematode growth media (NGM) plate and removing excess *E. coli* by washing with M9 buffer after pelleting worms and embryos by centrifuging for 7 seconds in a swinging bucket centrifuge (reaching a max speed of approximately 2000 RCF). The pellet was then treated with alkaline bleach wash to digest intact adults, freeing their eggs. The collected embryos are pelleted by centrifugation again for 7 seconds, and the pellet was washed 3 times with the supplemented L-15 media. We optimized eggshell digestion using yatalase[28] (T017, Takara Bio), but have found that more inexpensive sources of chitinase, such as from *S. griseus* (C6137, Sigma-Aldrich) also work well. Stock solutions of enzyme were prepared at 12.5 mg/mL in supplemented L-15 media and frozen in 10 μL aliquots. After thawing and warming to room temperature, 50 μL of the washed embryo suspension is added to the media and embryos are left to rock for up to 1 hour. The timing of visible eggshell digestion varies based on embryo density, with lower embryo density requiring shorter incubation times (85% in 60 minutes). Digested embryos were transferred by capillary micropipette into a 100 μL droplet of fresh media and covered in mineral oil to prevent evaporation and left overnight at room temperature (21-22 ℃).

After digestion, the eggshell is clearly missing when observed under high magnification DIC microscopy. Given the handling time needed to dissect early-stage embryos, transfer into yatalase and recover after digestion, we have not succeeded at reliably preparing the single cell

zygote in this manner. 2-cell embryos can be reliably isolated, digested and survive in L-15 + sucrose at rates comparable to later stage embryos (29/31). These early embryos digest quickly with 30% embryos having no visible eggshell within 5 minutes. To obtain the quickest digestion possible, roughly 30 embryos were added to the yatalase solution and immediately imaged under DIC to determine the timing of digestion. Pre-bean stage embryos show no visible remaining layers under DIC, but at comma stage, a flexible membrane becomes visible surrounding the embryo, which may be the peri-embryonic layer observed in electron micrographs of the eggshell[9]. Whether this membrane is formed at these stages or is simply too tightly bound to the embryo surface at earlier stages to be visible by DIC is unclear. After digestion, comma stage embryos will extend their tail less tightly folded and 3-fold embryos appear spherical rather than ovoid, both clear visual indications of complete digestion under low magnification observation. Upon completing embryonic development, L1 larvae are able to "hatch" from this soft membrane as normal (Fig 1A). We observe that >80% of early-stage embryos (younger than the bean stage and thus lacking an epidermis at the time of eggshell digestion) are able to survive and hatch as L1 (40/50) (Fig 1G). Many of the embryos that fail to hatch show signs of mechanical trauma, likely suffered during the capillary micropipette transfer process. We recovered a portion of the L1 larvae onto standard NGM plates seeded with OP50 *E. coli* and observed that >90% of those survived to become fertile adults (28/30) (Fig 1G). Late stage embryos are approximately as successful in reaching L1 (35/50) and becoming gravid adults (29/31), demonstrating that this minimal culture media is capable of maintaining embryo viability after eggshell removal at any stage of embryo development starting at the 2-cell stage and that animals treated in this fashion are fully capable of surviving and maturing to adulthood. The few larvae that are lost were not found arrested or dead, suggesting they were likely lost under the media or along the walls of the petri dish. Unsupplemented L-15 and standard egg buffer[29] yield a much lower rate of survival to L1 (45% (20/46, 27/53, 20/48) and 47% (9/17, 26/52, 24/56) respectively) with arrested embryos showing signs of severe osmotic stress such as swelling and bursting (Fig 1B-C).

We next optimized yatalase digestion duration and yield. By observing embryos in the chitinase solution periodically under DIC microscopy, we tracked the progression of eggshell digestion over time by observing when the eggshell is no longer visible. When digested in batches of 50 embryos in 2.5 mg/mL yatalase, just over half of the embryos are fully digested within 30 minutes with an increase to roughly 80% of embryos digested within 90 minutes (Fig 1F). Reducing the number of embryos to 20 per batch accelerated digestion, with 80% showing no visible eggshell within 60 minutes. It is likely that either inactivation of the yatalase or the increasing concentration of degraded chitin may be limiting the reaction. We tested this by replacing 20% of the chitinase suspension with fresh enzyme solution after 30 minutes of incubation and observed a marked increase in the ratio of digested embryos in large embryo preps (n> 100) 20 minutes following the addition of the enzyme. This strategy reduces the survival rate of embryos to 58% for early-stage embryos (29/50) and 54% for late-stage embryos (27/50) but of those that survived to L1 roughly 90% of both early and late-stage embryos became gravid adults (E=27/29, L=23/27). This drop in survival rates can likely be

attributed to the extra handling of the embryos and additional shear stresses during liquid exchange, as even partial eggshell digestion renders embryos extremely fragile.

Knockdown of *perm-1* using RNAi is commonly used to permeabilize early-stage embryos for small molecule treatment. Using the *perm-1* RNAi, we assayed survival in the culture conditions reported (0.7% egg salts) and saw that all (0/50) embryos tested failed to survive past the two-cell stage (Fig 1D). Culturing L15 + sucrose did not improve survival in *perm-1* RNAi with all embryos similarly arresting (0/50) (Fig 1E).

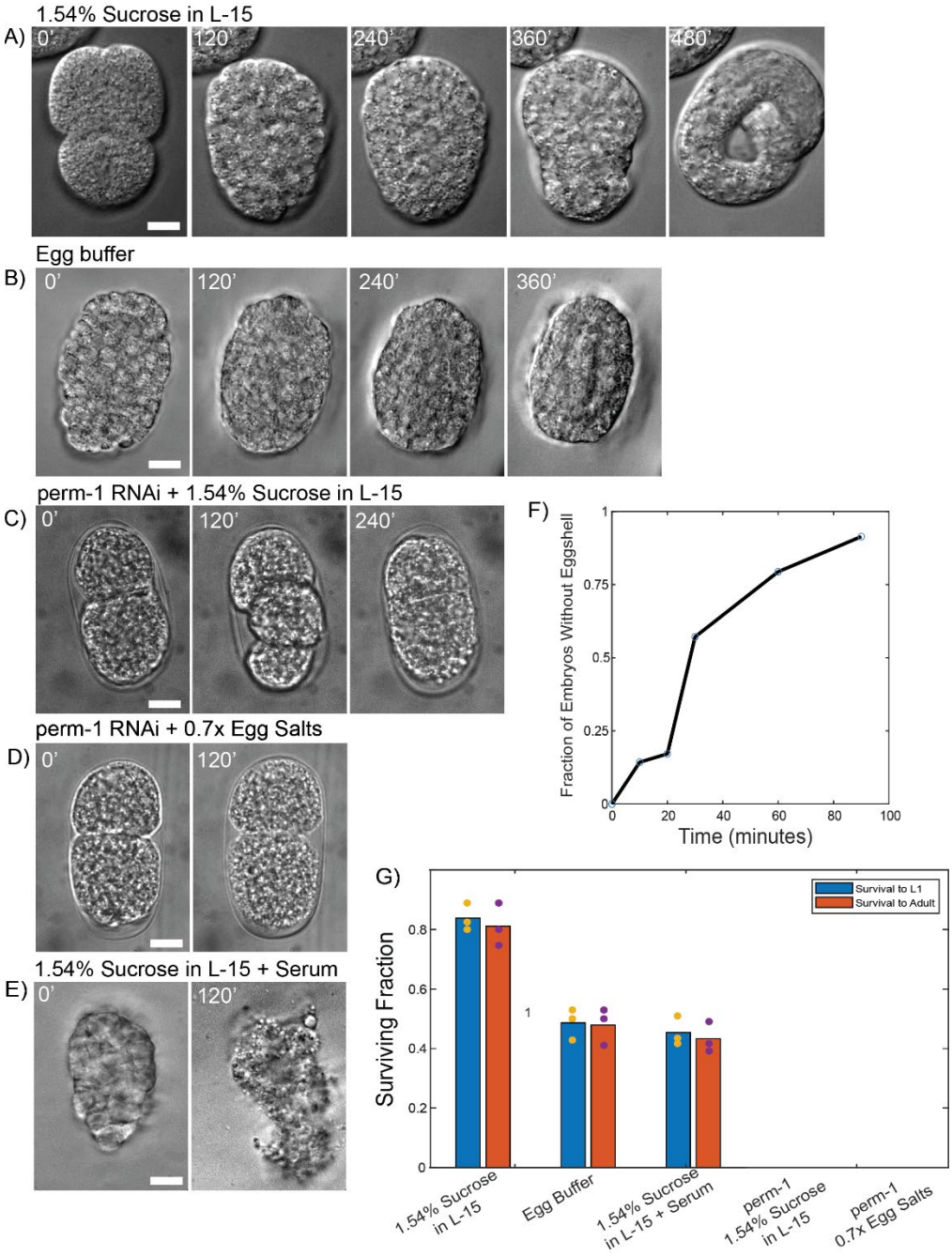

Figure 1. A) *ex ovo* embryos develop normally in 1.54% sucrose in L-15 (10 µm scale bar). B) *ex ovo* embryos show signs of osmotic stress when left in standard egg buffer and arrest (10 µm scale bar). C) perm-1 embryos cultured in 1.54% sucrose in L-15 (10 µm scale bar). D) perm-1 RNAi embryos in 0.7X Egg Salts (10 µm scale bar). E) *ex ovo* embryos in 1.54% sucrose L-15 media with serum quickly arrest and undergo apoptosis (10 µm scale bar). F) Time course of eggshell digestion in yatalase. Error bars show standard deviation of three replicates (with 18, 19 and 22 embryos in total each. G) Survival rates of *ex ovo* embryos cultured overnight in 1.54% sucrose in L-15, egg buffer, and serum supplemented L-15 media and perm-1 embryos in 1.54% sucrose in L-15 and in 0.7x Egg Salts. Blue bars show survival to L1 while orange bars show survival to fertile adulthood.

Ex ovo embryos are permeable to fluorescent dyes

Advances in synthetic chemistry continue to produce a wide range of small molecules that exhibit both desirable photophysical properties and selectivity to diverse subcellular compartments or sensitivity to variation in local environment. The loading of cell permeable dyes into the embryo has previously been achieved under genetic manipulation[9], chitinase digestion[27], coverslip pressure[19,20], or by feeding/injecting adults[30,31]. We reasoned that our eggshell digestion and embryo culture strategy would similarly render the embryo accessible to fluorescent dyes but in a manner compatible with long-term viability and imaging when combined with supplemented L-15 media.

Lysotracker[32] is a hydrophobic weak base that accumulates predominantly in acidic endosomes and lysosomes. This dye has been previously used in *C.elegans* studies to study gut granules and neuronal signaling in embryos and the adult worm by feeding worms on NGM plates with LysoTracker Red added for 12-48 h.[33] In *ex ovo* embryos cultured in L-15 media, Lysotracker rapidly stains all embryonic cells at all embryonic stages. At 100 nM, the manufacturer's suggested concentration for staining mammalian cells, LysoTracker Red exhibits a high level of toxicity as all stained embryos arrested after roughly 1 hour (n=9). At 10 nM, embryos developed normally and survived through elongation and twitching while acquiring sufficient dye to image with confocal microscopy. Labeled lysosomes (10nM) can be seen throughout the tissue with an increase in the number of lysosomes observed in the embryonic pharynx and intestine during early elongation (n=11) (Fig 2A). Embryos stain rapidly with detectable signal present less than one minute after dye addition.

While complete digestion of the eggshell provides several obvious visual cues, we next asked whether partial digestion could render the eggshell permeable. We added lysotracker concurrently with yatalase and observed the embryos by timelapse microscopy to determine when fluorescent staining first became visible (n=20 embryos per trial, repeated three times). Lysotracker became visible in 70% of embryos as soon as imaging began (<5 minutes post addition of dye, owing to the time required to mount the sample and begin timelapse imaging) with 80% of embryos staining after 30 minutes of digestion (Fig 2D). This rapid initial

permeabilization appears to be highly localized as often a small number of cells become stained initially followed by the diffusion of dye to more cells over time (Fig 2B). In these embryos the remaining eggshell accumulates some dye highlighting the incomplete digestion (Fig 2C).

We then replicated prior work staining neutral lipids in *C. elegans* embryos with a Boron-dipyrromethene (BODIPY) dye, using BDP™ 630/650 (Lumiprobe Corporation) to stain *ex ovo* embryos, examining the compatibility of this approach to live imaging. Boron-dipyrromethenes are a class of lipophilic fluorescent dyes used to stain cell membranes and lipid droplets[34]. Similar to LysoTracker Red, we see that BDP™ 630/650 at 0.5mg/mL rapidly labels all cells in *ex ovo* embryos with the images at T0 representing less than a minute after dye addition(n=12). As with prior work with chitinase-treated embryos[35], we observed both weak plasma membrane staining as well as enrichment of the dye in droplet-like structures. At the late comma stage coinciding with the terminal divisions of the endodermal E lineage (determined by nuclei positioning using H2B::mCherry), we observed a rapid enrichment of both LysoTracker Red and BDP™ 630/650 staining in the embryonic intestine (Fig 2E).

We replicated the experimental conditions to determine how quickly during digestion BDP 630/650 was able to infiltrate the embryo. BDP 630/650 showed a decrease in solubility in Yatalase suspension, as only 8% of embryos showed staining as soon as imaging started (<5 minutes after addition of dye and Yatalase) following which fluorescent droplets appeared in the media outside of embryos. After the appearance of dye droplets, no additional embryos showed signs of staining.

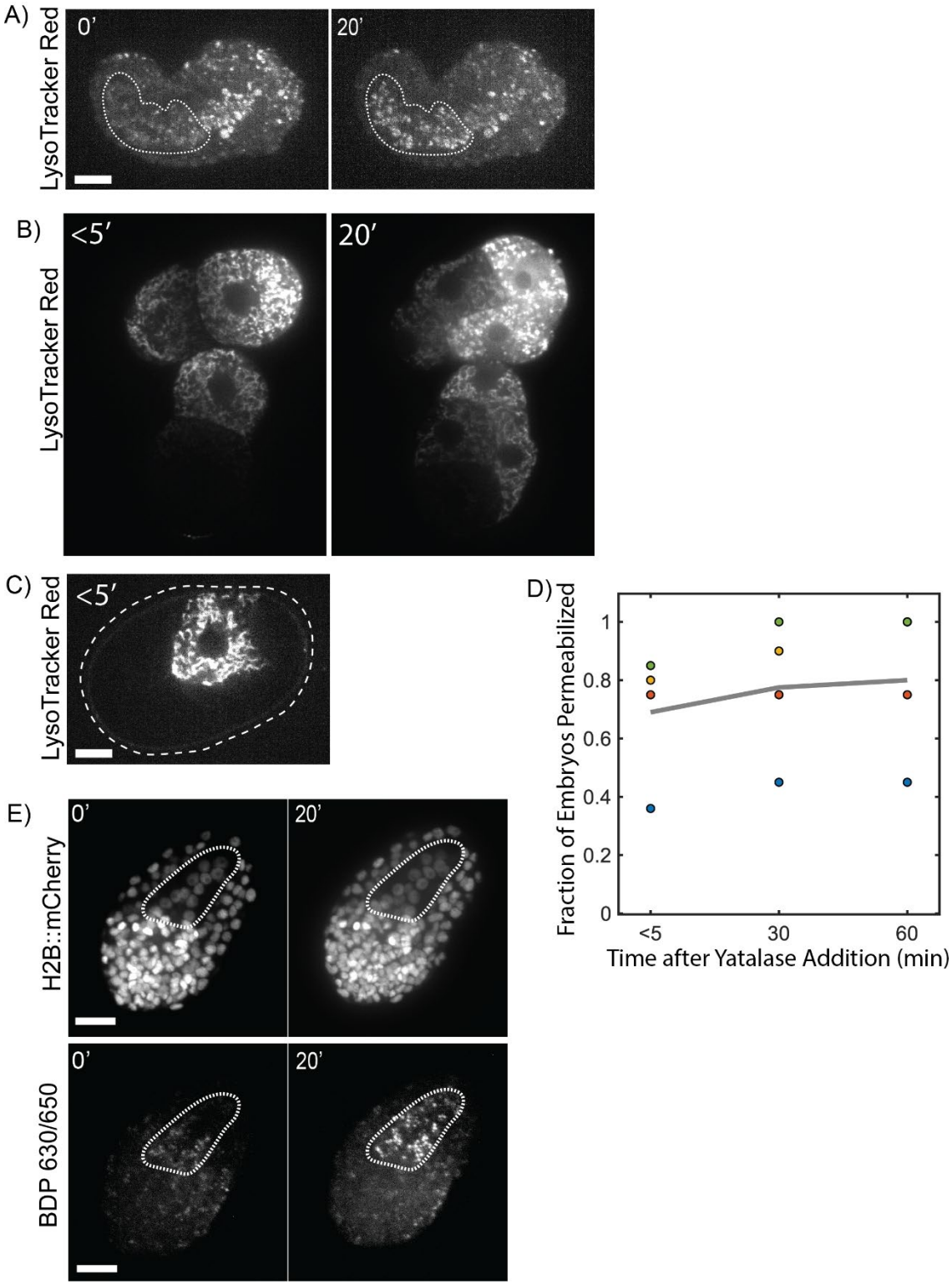

Figure 2. A) Maximum projection of *ex ovo* embryo stained with LysoTracker Red (10 µm scale bar). B) Time course showing staining of embryos using LysoTracker Red (10 µm scale bar). C) Embryo stained with LysoTracker Red (10µm scale bar). Dashed line to outline eggshell. D) Line plot showing the uptake of LysoTracker Red in actively permeabilizing embryos over time.

E) Maximum projection of *ex ovo* embryo stained with BDP 630/650 (10 µm scale bar). Dashed line outlines the embryonic intestine.

Manipulation of microtubule stability in *ex ovo* embryos

The microtubule cytoskeleton plays a critical structural and functional role in a wide range of fundamental cellular processes from mitosis[36] to morphogenesis[37]. Genetic and biochemical studies of *C. elegans* have identified a range of functional regulators of microtubules[38,39]. The essential role of microtubule regulation creates challenges for the study of the cytoskeleton at later developmental stages. The incomplete permeability barrier of the early single cell embryo and laser microbeam based permeabilization have previously been used to deliver microtubule toxins and drugs targeting microtubule regulators[10,40]. Given the accessibility of our cultured embryos to dyes, we reasoned that this approach would also make it possible to utilize microtubule toxins to manipulate the cytoskeleton at a wider range of developmental stages, without laser microbeam or coverslip pressure-assisted permeabilization.

Taxol functions by stabilizing microtubule filaments, preventing them from depolymerizing and stopping cell divisions causing mammalian cells to undergo apoptosis[41]. It has previously been used to study spindle axis establishment of the first cell division of the embryo in *C.elegans* and used as a control when testing new destabilizing treatments[40,42]. We tested a range of taxol doses in *ex ovo* embryos. Starting with a dose that had previously been used with *perm-1* RNAi treated embryos (100 nM)(n=13), the cells in embryos at all developmental stages immediately take on a spherical shape and arrest, with the same effect being seen at 50 nM (n=5). The addition of 100 nM taxol to embryos with intact eggshells caused no visible phenotype leading us to believe it is not able to penetrate the eggshell. Lower doses (10 nM) slowed the onset of complete stabilization treatment and allowed for the execution of a single post-treatment round of cell division to be completed before arresting completely, raising the possibility of studying the consequences of intermediate levels of microtubule stabilization (n=5) (Fig 3A). Using even lower doses (5 nM) (n=7), we observed a large increase in the amount of tubulin associated with the mitotic spindles in early-stage embryos, with the spindles pulled outward to the cell cortex (Fig 3B). At the lowest dose we tested (1 nM), cell divisions progressively slowed over the course of an hour until, regardless of embryo stage, all embryonic cell divisions stopped (n=5). In all cases, 100% of embryos lacking an eggshell based on DIC observation showed susceptibility to taxol.

Colchicine is a microtubule depolymerizer at high concentrations and a stabilizer at low concentrations[43]. In adult worms, colchicine has been used to disrupt dendritic microtubules in sensory neurons to determine their function in sensitivity to stimuli[44]. At 200 nM, a concentration used previously in *perm-1* RNAi treated embryos[10], embryonic cells rapidly became spherical and eventually burst (n=18) (Fig 3C). β-tubulin fluorescence in these embryos became

extremely diffuse and cytoplasmic compared to the cortical and spindle localization observed in untreated embryos. This concentration causes no visible phenotype in eggshell intact embryos (n=7). At a lower dose (10 nM) embryos after hypodermal enclosure continued development for a short period of time (roughly 30 mins) with β-tubulin becoming less localized at the cell cortex over time before the embryos arrested fully (n=7), while younger embryos showed the opposite phenotype with GFP::β-tubulin fluorescence increasing at the cell cortex and the embryos arresting immediately after treatment (n=9) (Fig 3D). At 1 nM, Colchicine mimicked the effects of Taxol treatment and appeared to stabilize microtubules at all developmental stages, causing a progressive accumulation of β-tubulin at mitotic spindles and a slowing of cell divisions leading to complete arrest within 30 minutes (n=17) (Fig 3B).

We then asked whether permeabilization of the eggshell to toxins was possible with incomplete digestion of the eggshell, similar to what we observed with lysotracker. We added 100 nM colchicine to the yatalase suspension and measured the amount of time it took for a phenotype to become apparent (slowing/stopping of cell divisions, decrease in cortical beta tubulin signal). While determining the precise timing of colchicine entry into the embryo is impossible in this case given the highly concentration-dependent phenotypes we previously observed, we tracked the earliest signs of abnormal microtubule dynamics we observed in these embryos, a doubling in the time required to complete cytokinesis (>4 minutes in treated embryos vs 2 minutes in untreated embryos), which became apparent within 10 minutes of digestion in 74% of embryos and all cell divisions in these embryos halted by 30 minutes post-drug addition in both 2-4 cell embryos and pregastrulation stage embryos (n=13). Embryos show a change in the localization of β-tubulin to the cytoplasm instead of the cell cortex within 15 minutes of drug addition (n=13). A portion of the embryos never showed any phenotype developing normally even in the presence of the small molecule, a similar fraction to those which do not show complete eggshell digestion in bulk (Fig 1F).

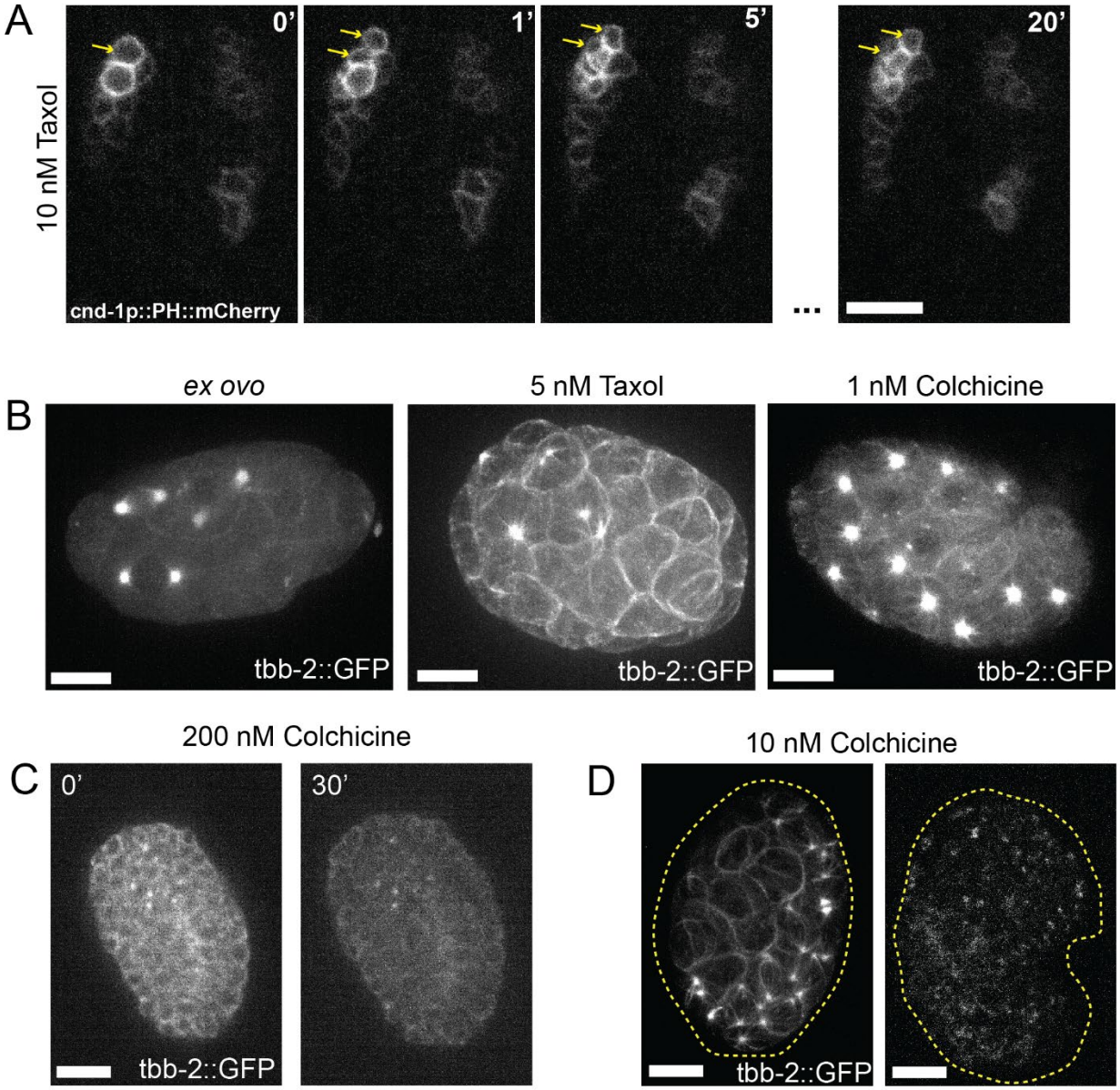

Figure 3. A) Maximum projections of cnd-1p::PH::mCherry embryos treated with 10 nM at the time of treatment, one minute post treatment, two minutes post treatment and twenty minutes post treatment. Yellow arrow heads pointing to cell division post treatment. B) Maximum projection of tbb-2::GFP early-stage *ex ovo* embryo in the absence of toxin (left). Maximum project of tbb-2::GFP early-stage embryo treated with 5 nM Taxol (middle). Maximum projection of tbb-2::GFP early-stage embryo treated with 1 nM of colchicine (right). Image intensity scaling is identical for all three images. C) Maximum projection of an tbb2::GFP embryo in the presence of 200 nM colchicine at the time of drug addition and 30 minutes post drug addition. Image intensity scaling is identical for both images. D) Maximum projection of early (left) and late (right) stage embryos tagged with tbb-2::GFP treated with 10 nM colchicine. Dashed line outlines the embryo. Image intensity scaling is identical for both images.

Manipulation of actin polymerization in *ex ovo* embryos

The actin cytoskeleton regulates many active processes in cell shape change and migration. The regulation of actin polymerization and branching generates mechanical anisotropies that direct a wide range of developmental events and has been extensively studied in the context of hypodermal enclosure in *C. elegans*[45,46]. Following gastrulation, hypodermal cells migrate towards the midline to enclose the embryo by extending actin-rich protrusions along the leading edge, which is unaffected in *ex ovo* embryos (protrusions marked by arrowheads) (n=10) (Fig 4A). Both the microtubule cytoskeleton and the assembly of contractile actin-myosin filaments are needed for proper enclosure. Embryos that fail to properly enclose typically rupture and arrest[46,47].

Jasplakinolide acts by binding to and stabilizing f-actin. It has been used to implicate F-actin contractile rings in the differentiation of spermatid[48]. In adults jasplakinolide has been used to study the relationship between the dynamic actin skeleton and the dynein motor proteins[49]. At high doses, matching its prior use in adult *C. elegans*, (500 nM), jasplakinolide treatment in embryos at the beginning of ventral enclosure blocked ventral migration and abolished ventral-oriented protrusions in the hypodermis of all treated embryos (Fig 4B) (n=7)[49]. Treating embryos with intact eggshells had no visible effect (9/9). Lower doses of Jasplakinolide (10 nM and 1 nM) also resulted in a complete block of ventral enclosure (n=12 and n=8 respectively).

Cytochalasin B is an inhibitor of actin polymerization by binding to F-actin and physically blocking filament extension. Laser ablation of the eggshell has previously been used to permeabilize the embryos to Cytochalasin B to determine actin's role in ventral enclosure and the migration of the leading cells[45]. The addition of 200 nM Cytochalasin B, the dose used previously in laser microbeam permeabilized embryos, to embryos with an intact eggshell at the beginning of ventral enclosure results in no visible phenotype (n=20)[19]. The lowest dose we tested (0.05 nM) also resulted in a fully penetrant failure of ventral enclosure (n=8) (Fig 4C).

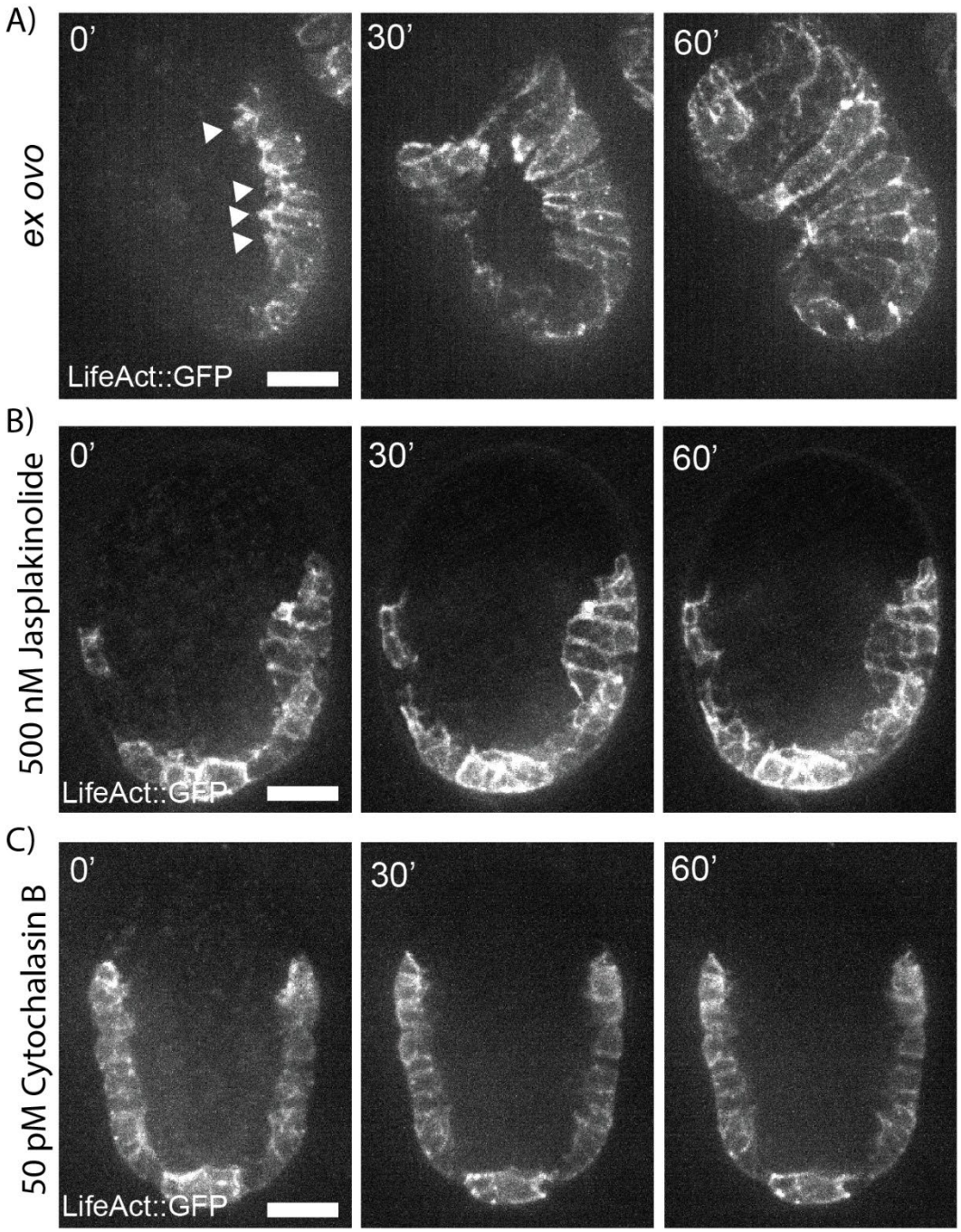

Figure 4. A) Maximum projection of the *ex ovo* embryos in the absence of drug. B) Maximum projection of *ex ovo* embryos following treatment of 500 nm Jasplakinolide. C) Maximum projection of *ex ovo* embryos following treatment of 0.05 nM Cytochalasin B.

The impacts of cytoplasmic dynein activity on the structure of the embryonic centrosome

Centrosomes must maintain integrity under the high levels of cortical stress applied during mitosis as it forms the mitotic spindle[50,51]. This structure is given to the centrosome by a fibrous protein matrix that surrounds the centriole called the pericentriolar material (PCM) providing strength to the organelle[52–54]. Cytoplasmic dynein plays an important role in shuttling proteins from the cytoplasm to the pericentriolar material to maintain centrosome integrity and to mediate centrosome duplication[55,56]. Previous studies have shown that inhibiting cytoplasmic dynein will cause cells to fail to divide and centrosomes will lose structural integrity leading to an increase in the size of the pericentriolar material[55,57,58].

Ciliobrevin D inhibits dynein's ATPase activity, thus blocking its processivity[59]. We treated *ex ovo* embryos with 10 nM Ciliobrevin D and tracked centrosome size using an endogenously tagged allele of PCMD-1[60]. We measured centrosome diameter by integrating the area under a uniformly sized line profile through 15 randomly selected centrosomes across 5 embryos 5 minutes prior to drug addition (-5 mins), immediately following drug addition (0 mins), and 5 minutes post-drug addition (+5 mins) (Fig A-B). We observed a significant increase in PCMD-1 area ($p= 4.9 \times 10^{-4}$ by the rank sum test)(Fig 5C).

Dynarrestin blocks the ability of dynein to bind to microtubules without affecting ATP hydrolysis[57]. We treated embryos with 10 nM Dynarrestin in the same manner as Ciliobrevin D and tracked centrosome size in 15 centrosomes across 5 embryos, 3 centrosomes per embryo (Fig 5B). Treated embryos show a significant increase in centrosome size immediately (<1 minute) following drug addition ($p= 0.003$, by rank sum test) as well as five minutes post drug addition ($p= 1.7 \times 10^{-5,}$ by rank sum test) (stars denote significance) (Fig 5C).

Prior work across cell culture, mammalian neurons, *Drosophila* neuroblasts and *C.elegans* sensory neurons have demonstrated that the minus end directed microtubule motor protein dynein is necessary for transport of the centrosome to the site of ciliogenesis. Loss of cytoplasmic dynein in these systems results in the centrosome remaining in the cell body and a failure of ciliogenesis. In *C. elegans,* a subset of sensory neurons executes a terminal division after the neuroblast extends a dendrite[61]. In these cells, the centrosome translocates from the cell body to the sensory ending following this division (Fig 5F). Prior work established a role for dynein in centriole transport during dendrite morphogenesis, relying on bulk heat shock-induced targeted mutagenesis of the dynein heavy chain *dhc-1*, and then assessing larval animals for basal body positioning defects[62]. We asked whether dynein activity is similarly required for long-range transport of the centrosome in embryonically born sensory neurons using *ex ovo* embryos and a small molecule inhibitor of dynein. We took advantage of the rapid onset of phenotypes following dynein inhibition by precisely timing the addition of 100 nM Dynarrestin just following the completion of the URX terminal division. We then tracked the centrosome up until the onset

of embryonic twitching using an endogenously tagged allele of PCMD-1 (Fig 5F). In almost all embryos treated in this manner (17/18), we observed that the centriole arrested motion within the cell body and failed to migrate along the dendrite before the onset of twitching (Fig 5G).

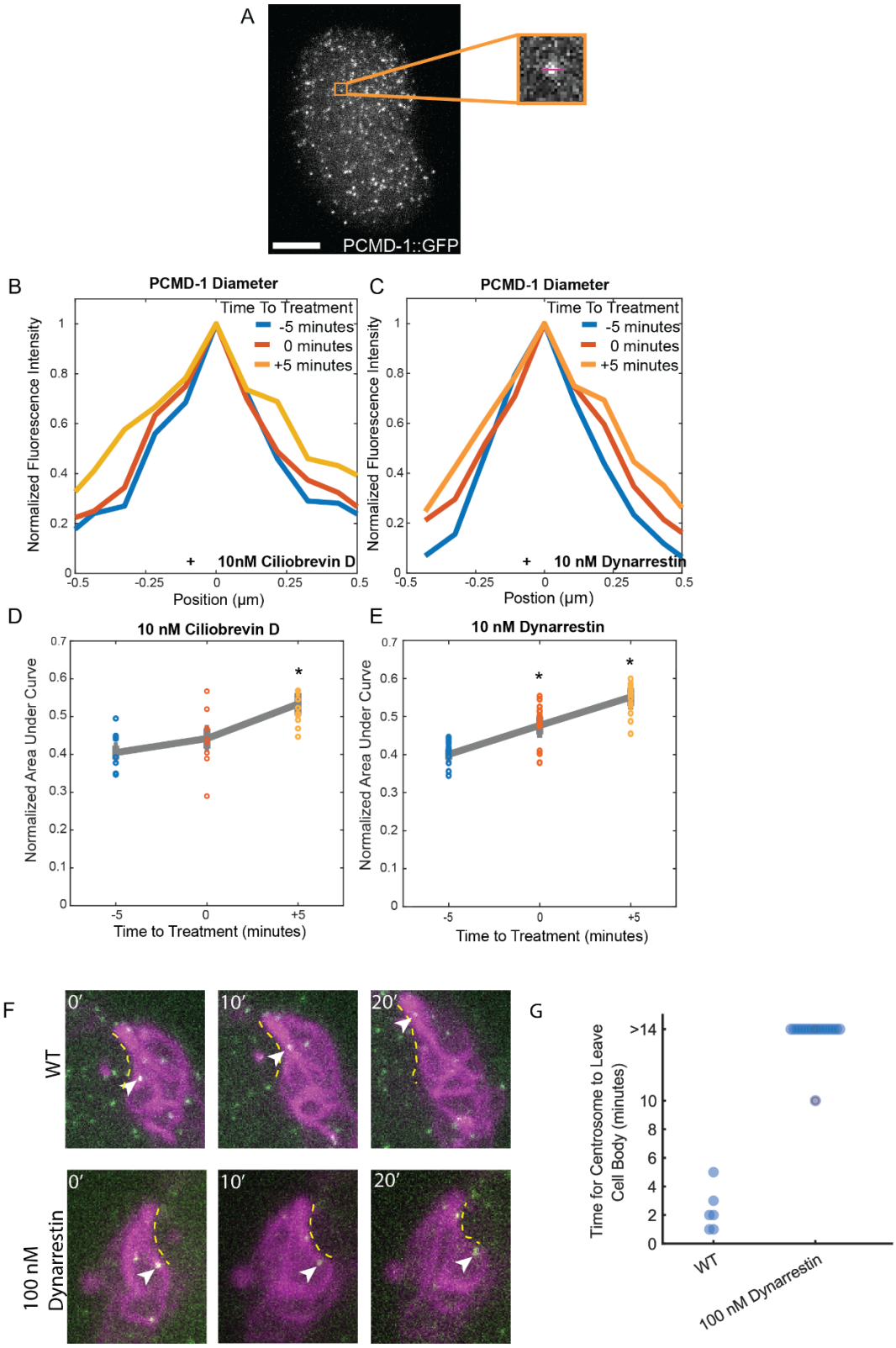

Figure 5. A) maximum projection of PCMD-1::GFP embryo. Inset showing one centrosome with a line through to demonstrate the line scan measurements taken. B) Line plot of PCMD-1

diameter for ciliobrevin D at five minutes before drug addition (blue), at the time of drug addition (orange) and five minutes post drug addition (yellow). Stars denote significance. C) Line plot of PCMD-1 diameter for Dynarrestin at five minutes before drug addition (blue), at the time of drug addition (orange) and five minutes post drug addition (yellow). Stars denote significance. D) Swarm plots of the normalized area under the curve for ciliobrevin at five minutes before drug addition (blue), at the time of drug addition (orange) and five minutes post drug addition (yellow). Stars denote significance. E) Swarm plots of the normalized area under the curve for Dynarrestin at five minutes before drug addition (blue), at the time of drug addition (orange) and five minutes post drug addition (yellow). Stars denote significance. F) Inset time course showing the progression of the centrosome along the dendrite in both untreated permeabilized embryos and permeabilized embryos treated with 100 nM dynarrestin. Arrowheads to denote centrosome and dashed lines to show dendrite. G) Swarm plot showing time for centrosomes to leave the cell body and enter the dendrite in both untreated and 100 nM Dynarrestin permeabilized embryos. Embryos at greater than 14 minutes had centrosomes that were never observed leaving the cell body before the onset of twitching which occurs 14- 30 minutes following the terminal division of the neuron.

Discussion

The study of cell and developmental biology has long made use of an assorted toolkit of highly specific toxins, inhibitors, and fluorescent dyes to manipulate and illuminate molecular processes *in vivo*. The impermeability of the *C. elegans* eggshell has limited the adoption of these tools for the study of developmental processes, motivating several efforts to overcome these limitations. The discovery of *perm-1,* and its inhibition by RNAi to render the early embryo permeable to small molecules was a revolutionary step forward in this field and has been used to dissect diverse processes in early embryonic development. Despite its utility in studying events in early-stage embryos, the inability of *perm-1* RNAi embryos to develop beyond gastrulation has prevented its use in later stages of embryogenesis such as in the study of tissue morphogenesis or neuronal cell biology. Our determination that simplified cell culture media support an exceptional level of embryo viability after eggshell removal through to larval development and adulthood provides a useful route forward for the introduction of these tools to the cell and developmental biologist lacking access to laser microbeams for targeted permeabilization, while reducing variability in preparation compared to the application of excess coverslip pressure. Given the high viability of *ex ovo* embryos cultured in this manner, permeabilization can take place well in advance of any developmental timepoint of interest, allowing for precisely timed drug addition for acute perturbations.

We demonstrated the compatibility of cultured *ex ovo* embryos with fluorescent labeling using LysoTracker Red and BDP 630/650, dyes that allow for the real-time characterization of physiological processes. In examining dye diffusion during eggshell digestion, we found that a subset of embryos showed signs of localized permeabilization of the eggshell with a distinct

“entry point” of dye followed by gradual diffusion and equilibration through the rest of the embryo, a phenomenon we did not observe during dye addition following complete eggshell digestion. Whether highly localized mechanical perturbation strategies such as laser ablation or the application of coverslip pressure generate similar internal gradients in acute drug treatments is unclear but potentially of concern to users of these methods.

Cytoskeletal manipulations have been a major focus of prior strategies for eggshell permeabilization given the challenges involved in genetic manipulation of microtubule and actin networks. We found that cultured *ex ovo* embryos are highly compatible with a range of commonly used toxins, often showing robust phenotypes at 0.1-1% of dosages reported in previous reports in *perm-1* RNAi, laser microbeam, and coverslip pressure permeabilized embryos. This allowed us to explore a wide range of dosages, finding potentially interesting stage and dose-dependent effects of Colchicine in contrast to the relatively invariant and potent effects of Taxol. Higher doses of Colchicine (200 nM) robustly produced phenotypes consistent with microtubule destabilization, including loss of cortical localization and subsequent rounding of cells. An intermediate dose (10 nM) showed signs of opposing effects in a stage-dependent manner where gastrulation-stage embryos showed signs of stabilization with increasing intensity of GFP-tagged tubulin at the cortex and spindle, whereas comma stage embryos showed phenotypes consistent with destabilization, just as with higher doses. At the lowest dose we tested (1 nM) we observe consistent, stage-independent signs of stabilization, yet only of spindle-associated microtubules, not in microtubules at the cell cortex. Whether this reflects stage-dependent variation in the utilization of tubulin isotypes or size and mechanical force-dependent effects of the drug is unclear. Our experiments with actin-interacting drugs including the stabilizer Jasplakinolide and destabilizer Cytochalasin B showed highly potent phenotypes at all doses tested, rapidly arresting ventral enclosure of the hypodermis and generally abolishing actin rich protrusions at the leading edge of the enclosing tissue, in close agreement with prior work using mechanical permeabilization to study this process[45,46].

We used *ex ovo* embryos in combination with two complementary inhibitors of dynein to probe the role of cytoplasmic dynein in the structure of the pericentriolar material, a highly structured proteinaceous matrix that confers microtubule organization functionality to the centriole[63,64], and the transport of the centriole to the sensory ending of ciliated neurons during embryonic development. Dynein plays a critical role in trafficking PCM components to the centrosome and maintaining the density of the PCM shell[56] and inhibition of cytoplasmic dynein has previously been shown to result in an expansion of the PCM as this internally directed force is removed[55,57]. Consistent with this function, we observed a steady increase in the diameter of centrioles visualized using an endogenously GFP tagged allele of PCMD-1 following addition of either Ciliobrevin D, which acts by inhibiting the ATPase domain of dynein, or Dynarrestin, which interferes with dynein’s ability to bind microtubules.

Ciliated sensory neurons rely on their primary cilia, which is most often localized to a dendritic ending, to transduce sensory input. In some cases this occurs during the morphogenesis of the neuron, in *C. elegans* a noncanonical microtubule organizing center exists at the tip of the growth cone while an inactive centriole is towed just behind the extending tip[65]. In the post embryonically-derived PQR neuron, it was shown that perturbation of dynein resulted in the disruption of this towing and the loss of a basal body at the distal tip of the dendrite[62]. Mammalian olfactory sensory neurons (OSNs) elaborate large networks of dendrites requiring centrioles to be transported long distances to the apical surface for the formation of primary cilia and dynein has been hypothesized to play a role in this transport[66]. Similar to mammalian OSNs, a subset of *C.elegans* sensory neurons extend a primary dendrite prior to their terminal division, requiring the centrosome to be transported along this pre-existing process to the site of ciliogenesis[61]. In these cells, the post-mitotic centriole is rapidly loaded into the dendrite, within 5 minutes of division. Given the rapidity with which our acute treatments with dynein inhibitors induced visible changes in PCM structure, we sought to target this narrow window between the completion of cytokinesis in sensory neurons and the beginning of the centriole's migration along the dendrite. Dynein inhibition before the completion of terminal division blocks cytokinesis, making it necessary to employ acute, precisely timed treatments. Live imaging during acute treatment showed that treatment with 100 nM Dynarrestin results in a highly penetrant block of centriole transport with treated embryos retaining their centriole in the cell body at the onset of embryo twitching, which occurred between 14 and 30 minutes after this terminal division.

We have demonstrated that a wide range of dyes and drugs work effectively in these culture conditions at picomolar to nanomolar concentrations, often far lower than has been demonstrated via other permeabilization strategies. Embryos cultured using this approach are not only viable but develop normally and are able to generate viable progeny, a marked improvement over *perm-1* RNAi, which compromises embryo viability beyond gastrulation, and without the potential acute mechanical stressors of laser microbeam and coverslip pressure induced permeabilization. Since eggshell digestion is scalable, large pools of *ex ovo* embryos can be easily prepared from transgenic, mutant, or RNAi-fed strains. The generation of *ex ovo* embryos and their stable long-term culture will be a useful tool for cell and developmental biology, expanding the accessibility of molecular tools in the study of *C. elegans* embryonic development.

Acknowledgements

This work was supported by NIH grant R35GM151199 to PKS. CAS was supported in part by NIH grant T32GM145388. Some strains were provided by the CGC, which is funded by NIH Office of Research Infrastructure Programs (P40OD010440). zyIs36 was a gift of Antonio Colavita. The RNAi library was provided by Patrick Allard. The authors would like to thank Jorge Torres and Margot Quinlan for the gift of reagents used in this study and valuable discussion.

Methods

***C. elegans* strains**

Strain	Genotype	Source
FT1197	xnIs449 [lin-26::lifeAct::GFP + unc-119(+)]	CGC
N2		CGC
JH2054	axIs1492 [pie-1p::GFP::tbb-2 ORF::tbb-2 3'utr + unc-119(+)]	CGC
TMD119	pcmd-1(syb486[gfp::pcmd-1]) I	CGC
zyIs36	zyIs36 [cnd-1p::PH::mCherry; myo-2p::mCherry] X	Shah & Tanner *et al.* 2017[52]
PKS19	zyIs36, unc-119(ed3) III; axIs1492.	This paper
PKS27	zyIs36, pcmd-1(syb486[gfp::pcmd-1]) I	This paper

Embryo collection

Supplemented media was prepared by dissolving 7.7 g sucrose into a 500 mL bottle of commercial L-15 media to a final concentration of 1.54% sucrose in L-15 media. The supplemented media was stored in 10 mL aliquots frozen at -20 °C. At this temperature, the media did not appear to degrade over time (for a period of at least 6 months). After thawing, if the media was used for long-term culture experiments (longer than approximately 2–3 hours), penicillin/streptomycin (100 units/mL final concentration) was added. Adding antibiotics prior to freezing resulted in precipitation that could interfere with imaging but did not appear to affect embryo viability.

Adult worms were seeded onto an NGM media plate for at least two days to obtain enough embryos. The plate containing embryos was washed off by pipetting 3000 µL M9 buffer and collecting it into a 15 mL centrifuge tube. The buffer was repeatedly drawn up and ejected onto the plate to completely collect worms. If residual worms and embryos remained on the plate post-washing, an additional 1000 µL of M9 was used. Enough M9 buffer was then added to the centrifuge tube containing worms and embryos to reach the 5 mL line. The contents were

vortexed and centrifuged at 2,000 rpm (600 rcf) for 6 seconds to gently pellet the worms and embryos. The supernatant was aspirated down to the 1–2 mL line, taking care not to disturb the pellet. The pellet was washed again with 5 mL M9 solution three times as described above to remove bacteria.

5 mL of M9 buffer was added to the pellet. Then, 250 µL of 10-15% NaOCl (Millipore Sigma #425044) and 125 µL of 5N NaOH were added. The tube was vortexed in 30–60 second increments for 1–2 minutes. Embryos were pelleted by centrifuging at 2.0 rpm for 1 minute. The supernatant was aspirated, taking care not to disturb the pellet, and another round of the bleaching process was performed as described. After each vortexing step, the sample was checked under a dissection scope to confirm whether embryos were released from gravid adults and all worms fully digested to minimize debris carried over into subsequent steps. The bleached embryos were washed with 5 mL of the supplemented L-15 media three times to ensure complete removal of bleach.

Eggshell digestion and embryo culture

After the final wash, embryos were pelleted again and excess media was removed. 50 µL of the embryos remaining were transferred to a microcentrifuge tube, followed by 10 µL of 12.5 mg/mL Yatalase (Takara T017). If processing fewer than 100-200 embryos, a single 10 µL Yatalase aliquot was added and incubated on a rocking rack for 1 hour before proceeding. If processing up to approximately 500 embryos, the suspension was incubated for 20 minutes while rocking after the first 10 µL Yatalase addition and then left to stand for 10 minutes to allow the pellets to settle by gravity. Then, 10 µL of supernatant was carefully pipetted from the surface and examined under a microscope for the presence of embryos. If no embryos were observed, a total of 15 µL of the supernatant was removed. A second 10 µL Yatalase aliquot was then added to the tube and mixed by pipetting up and down. The sample was not vortexed at this stage, as partial digestion from the first Yatalase addition makes embryos fragile and prone to rupture. The embryos were incubated with the second Yatalase treatment for another 20 minutes on the rocking rack. After this stage, we do not wash the remaining Yatalase from the solution to minimize handling.

To verify the viability of *ex ovo* embryos, we transfer 10-20 embryos into 50 µL of fresh media in a 35 mm petri dish, cover the droplet with mineral oil to prevent evaporation, and leave the embryos at room temperature overnight, scoring survival based on the appearance of swimming L1 larvae the following morning.

RNAi

For feeding the RNAi, a clone of T01H3.4 from the Ahringer library was grown in 200ul of LB + carbenicillin overnight at 37C[53]. 100ul of bacterial culture was added to each of the IPTG plates and left to dry overnight. 20-40 L4 or young adult stage worms were added to each plate and left in a 20C incubator overnight.

For imaging, worms were transferred to a microwell slide in 50ul of 0.7x Egg Salts (1X Egg Salts: 118 mM NaCl, 40 mM KCl, 3.4 mM MgCl2, 3.4 mM CaCl2, 5 mM HEPES pH 7.4)[54]. 5 worms were cut using a scalpel and an eyelash was used to separate out 2-4 cell embryos. Those embryos were transferred to 24x 50 mm coverslips and mounted using ~5ul of 0.7x Eggsalts with 20um beads. A top coverslip was placed and the edges sealed with vaseline. Embryos were imaged for 4 hours on Olympus IX83 inverted microscope frame, a UPSAPO 60XS2 silicone oil immersion objective and a VisiTech iSIM super resolution multipoint scanning confocal microscope. The same process was repeated but with 1.54% sucrose in L15 media.

Light microscopy

Ex ovo embryos are extremely fragile mechanically and care should be taken to minimize direct manipulation but are compatible with standard nematode embryo mounting practices such as bead-based compression mounting. Compression mounting with agar pads invariably results in the destruction of the embryos and should be avoided. Uncoated chambered coverslips (µ-Slide, ibidi GmbH) were used in cases where the timing of drug introduction is desirable for temporal control of treatments for inverted high-resolution imaging.

All imaging was performed using an Olympus IX83 inverted microscope frame, a UPSAPO 60XS2 silicone oil immersion objective and a VisiTech iSIM super resolution multipoint scanning confocal microscope.

Image processing

Unless otherwise noted, no background subtraction or post-processing beyond linear contrast and brightness adjustment in Fiji was performed. Lysotracker imaging at low concentrations was prone to photobleaching so an exponential fit using Fiji's bleach correction plugin was used to process these images.

Bead mounting for imaging with inverted microscopes

Ex ovo embryos tolerate compressed mounting using methods previously optimized for imaging during long-term time lapse for cell lineage tracing[55]. Briefly, a suspension of 20 µm diameter polystyrene beads (Thermo Scientific 09-980-133) is prepared in L-15 media with sucrose and antibiotics. This preparation is diluted empirically to achieve a final concentration of 100-200

beads per μL. For imaging, *ex ovo* embryos are transferred into a 2 μL drop of bead suspension on a #1.5 coverslip by capillary micropipette. A smaller coverslip is placed on top and secured in place by painting with melted petroleum jelly without moving the coverslip after placement to avoid damaging the embryos. Imaging post-twitching embryos in this format is made challenging as the lack of a rigid eggshell allows *ex ovo* embryos to generate traction against the coverslip surfaces and migrate slowly.

Open mounting for accessibility for drug delivery

While bead-compressed mounting is advantageous for numerous applications, the closed nature of the preparation complicates acute addition of small molecules. For the timed treatment of embryos with the dynein inhibitors Dynarrestin and Ciliobrevin D, we used open-chambered slides (ibidi 80821) to mount embryos. Mounting embryos in 50 μL of media and diluting additives to 100⨯ stock concentrations to reduce the volume of the added drug minimized disruption to the embryo positions during time lapse imaging, allowing for precisely timed drug addition.

References

1. Shah, P., Bao, Z. & Zaidel-Bar, R. Visualizing and quantifying molecular and cellular processes in Caenorhabditis elegans using light microscopy. *Genetics* 221, iyac068 (2022).

2. Breimann, L., Preusser, F. & Preibisch, S. Light-microscopy methods in C. elegans research. *Curr. Opin. Syst. Biol.* 13, 82–92 (2019).

3. Wang, S. *et al.* A toolkit for GFP-mediated tissue-specific protein degradation in C. elegans. *Development* 144, 2694–2701 (2017).

4. Zhang, L., Ward, J. D., Cheng, Z. & Dernburg, A. F. The auxin-inducible degradation (AID) system enables versatile conditional protein depletion in C. elegans. *Development* 142, 4374–4384 (2015).

5. Davis, L. *et al.* Precise optical control of gene expression in C elegans using improved genetic code expansion and Cre recombinase. *eLife* 10, e67075 (2021).

6. Henau, S. D., Pagès-Gallego, M., Pannekoek, W.-J. & Dansen, T. B. Mitochondria-Derived H2O2 Promotes Symmetry Breaking of the C. elegans Zygote. *Dev. Cell* 53, 263-271.e6 (2020).

7. Churgin, M. A., He, L., Murray, J. I. & Fang-Yen, C. Efficient Single-Cell Transgene Induction in Caenorhabditis elegans Using a Pulsed Infrared Laser. *G3 GenesGenomesGenetics* 3, 1827–1832 (2013).

8. Singhal, A. & Shaham, S. Infrared laser-induced gene expression for tracking development and function of single C. elegans embryonic neurons. *Nat. Commun.* 8, 14100 (2017).

9. Olson, S. K., Greenan, G., Desai, A., Müller-Reichert, T. & Oegema, K. Hierarchical assembly of the eggshell and permeability barrier in C. elegans. *J. Cell Biol.* 198, 731–748 (2012).

10. Carvalho, A. *et al.* Acute Drug Treatment in the Early C. elegans Embryo. *PLOS ONE* 6, e24656 (2011).

11. Dong, L. *et al.* Integrated Microfluidic Device for Drug Studies of Early C. Elegans Embryogenesis. *Adv. Sci.* 5, 1700751 (2018).

12. Winkenbach, L. P., Parker, D. M., Williams, R. T. P. & Nishimura, E. O. The ERM-1 membrane-binding domain directs erm-1 mRNA localization to the plasma membrane in the C. elegans embryo. *Dev. Camb. Engl.* 149, dev200930 (2022).

13. Torisawa, T., Saito, K., Furuta, K. & Kimura, A. Active fluctuations of cytoplasmic actomyosin networks facilitate dynein-driven intracellular transport along microtubules. 2024.05.23.595269 Preprint at https://doi.org/10.1101/2024.05.23.595269 (2024).

14. Ellenbecker, M. & Voronina, E. Disruption of C. elegans embryonic P granules upon dlc-1(RNAi) is not associated with P granule component loss. *MicroPublication Biol.* 2022, 10.17912/micropub.biology.000700.

15. Maheshwari, R. *et al.* A membrane reticulum, the centriculum, affects centrosome size and function in Caenorhabditis elegans. *Curr. Biol.* 33, 791-806.e7 (2023).

16. González, D. P. *et al.* CBD-1 organizes two independent complexes required for eggshell vitelline layer formation and egg activation in C. elegans. *Dev. Biol.* 442, 288–300 (2018).

17. Severson, A. F., Baillie, D. L. & Bowerman, B. A Formin Homology Protein and a Profilin Are Required for Cytokinesis and Arp2/3-Independent Assembly of Cortical Microfilaments in *C. elegans*. *Curr. Biol.* 12, 2066–2075 (2002).

18. Skop, A. R., Bergmann, D., Mohler, W. A. & White, J. G. Completion of cytokinesis in *C. elegans* requires a brefeldin A-sensitive membrane accumulation at the cleavage furrow apex. *Curr. Biol.* 11, 735–746 (2001).

19. Hill, D. P. & Strome, S. Brief cytochalasin-induced disruption of microfilaments during a critical interval in 1-cell C. elegans embryos alters the partitioning of developmental instructions to the 2-cell embryo. *Dev. Camb. Engl.* 108, 159–172 (1990).

20. Edgar, L. G. & McGhee, J. D. DNA synthesis and the control of embryonic gene expression in C. elegans. *Cell* 53, 589–599 (1988).

21. Brennan, L. D. *et al.* Small Molecule Injection into Single-Cell C. elegans Embryos via Carbon-Reinforced Nanopipettes. *PLOS ONE* 8, e75712 (2013).

22. Shelton, C. A. & Bowerman, B. Simplified embryonic growth medium for *Caenorhabditis elegans*. *Tech. Tips Online* 3, 46–47 (1998).

23. Manzi, N. I., de Jesus, B. N., Shi, Y. & Dickinson, D. J. Temporally distinct roles of Aurora A in polarization of the C. elegans zygote. *bioRxiv* 2023.10.25.563816 (2023) doi:10.1101/2023.10.25.563816.

24. Stolpner, N. J., Manzi, N. I., Su, T. & Dickinson, D. J. Apical PAR protein caps orient the mitotic spindle in C. elegans early embryos. *Curr. Biol. CB* 33, 4312-4329.e6 (2023).

25. Edgar, L. G. & Goldstein, B. Culture and Manipulation of Embryonic Cells. *Methods Cell Biol.* 107, 151–175 (2012).

26. Christensen, M. *et al.* A Primary Culture System for Functional Analysis of *C. elegans* Neurons and Muscle Cells. *Neuron* 33, 503–514 (2002).

27. Schmökel, V. *et al.* Genetics of Lipid-Storage Management in Caenorhabditis elegans Embryos. *Genetics* 202, 1071–1083 (2016).

28. Wu, Y. *et al.* Multiview confocal super-resolution microscopy. *Nature* 600, 279–284 (2021).

29. Zhang, S. & Kuhn, J. R. Cell isolation and culture. in *WormBook: The Online Review of C. elegans Biology [Internet]* (WormBook, 2018).

30. Boyd, L., Hajjar, C. & O'Connell, K. Time-lapse Microscopy of Early Embryogenesis in Caenorhabditis elegans. *J. Vis. Exp. JoVE* 2852 (2011) doi:10.3791/2852.

31. Chang, Y. & Dickinson, D. J. Non-invasive chimeric HaloTag labeling to study clustering and diffusion of membrane proteins. *STAR Protoc.* 3, 101857 (2022).

32. Zhitomirsky, B., Farber, H. & Assaraf, Y. G. LysoTracker and MitoTracker Red are transport substrates of P-glycoprotein: implications for anticancer drug design evading multidrug resistance. *J. Cell. Mol. Med.* 22, 2131–2141 (2018).

33. Genetic Analysis of Lysosomal Trafficking in Caenorhabditis elegans - PMC. https://pmc.ncbi.nlm.nih.gov/articles/PMC1165410/.

34. Listenberger, L. L. & Brown, D. A. Fluorescent Detection of Lipid Droplets and Associated Proteins. *Curr. Protoc. Cell Biol.* 35, 24.2.1-24.2.11 (2007).

35. Metabolic plasticity sustains the robustness of Caenorhabditis elegans embryogenesis - PMC. https://pmc.ncbi.nlm.nih.gov/articles/PMC10702823/.

36. Toya, M., Iida, Y. & Sugimoto, A. Imaging of Mitotic Spindle Dynamics in *Caenorhabditis elegans* Embryos. in *Methods in Cell Biology* (eds Cassimeris, L. & Tran, P.) vol. 97 359–372 (Academic Press, 2010).

37. Shaye, D. D. & Greenwald, I. The Disease-Associated Formin INF2/EXC-6 Organizes Lumen and Cell Outgrowth during Tubulogenesis by Regulating F-Actin and Microtubule Cytoskeletons. *Dev. Cell* 32, 743–755 (2015).

38. Al-Bassam, J. & Chang, F. Regulation of microtubule dynamics by TOG-domain proteins XMAP215/Dis1 and CLASP. *Trends Cell Biol.* 21, 604–614 (2011).

39. Bot, N. L., Tsai, M.-C., Andrews, R. K. & Ahringer, J. TAC-1, a Regulator of Microtubule Length in the C. elegans Embryo. *Curr. Biol.* 13, 1499–1505 (2003).

40. Hyman, A. A. & White, J. G. Determination of cell division axes in the early embryogenesis of Caenorhabditis elegans. *J. Cell Biol.* 105, 2123–2135 (1987).

41. Lim, P. T., Goh, B. H. & Lee, W.-L. 3 - Taxol: Mechanisms of action against cancer, an update with current research. in *Paclitaxel* (eds Swamy, M. K., Pullaiah, T. & Chen, Z.-S.) 47–71 (Academic Press, 2022). doi:10.1016/B978-0-323-90951-8.00007-2.

42. Bajaj, M. & Srayko, M. Laulimalide Induces Dose-Dependent Modulation of Microtubule Behaviour in the C. elegans Embryo. *PLoS ONE* 8, e71889 (2013).

43. Schlesinger, N., Firestein, B. L. & Brunetti, L. Colchicine in COVID-19: an Old Drug, New Use. *Curr. Pharmacol. Rep.* 6, 137–145 (2020).

44. Bounoutas, A. *et al.* Microtubule depolymerization in Caenorhabditis elegans touch receptor neurons reduces gene expression through a p38 MAPK pathway. *Proc. Natl. Acad. Sci. U. S. A.* 108, 3982–3987 (2011).

45. Williams-Masson, E. M., Malik, A. N. & Hardin, J. An actin-mediated two-step mechanism is required for ventral enclosure of the C. elegans hypodermis. *Development* 124, 2889–2901 (1997).

46. Williams-Masson, E. M., Heid, P. J., Lavin, C. A. & Hardin, J. The Cellular Mechanism of Epithelial Rearrangement during Morphogenesis of the*Caenorhabditis elegans*Dorsal Hypodermis. *Dev. Biol.* 204, 263–276 (1998).

47. Sulston, J. E., Schierenberg, E., White, J. G. & Thomson, J. N. The embryonic cell lineage of the nematode *Caenorhabditis elegans*. *Dev. Biol.* 100, 64–119 (1983).

48. Hu, J. *et al.* Distinct roles of two myosins in C. elegans spermatid differentiation. *PLOS Biol.* 17, e3000211 (2019).

49. Gil-Krzewska, A. J., Farber, E., Buttner, E. A. & Hunter, C. P. Regulators of the Actin Cytoskeleton Mediate Lethality in a Caenorhabditis elegans dhc-1 Mutant. *Mol. Biol. Cell* 21, 2707–2720 (2010).

50. Enos, S. J., Dressler, M., Gomes, B. F., Hyman, A. A. & Woodruff, J. B. Phosphatase PP2A and microtubule-mediated pulling forces disassemble centrosomes during mitotic exit. *Biol. Open* 7, bio029777 (2018).

51. Mittasch, M. *et al.* Regulated changes in material properties underlie centrosome disassembly during mitotic exit. *J. Cell Biol.* 219, (2020).

52. Jha, K., Woglar, A., Busso, C., Hatzopoulos, G. N. & Gönczy, P. C. elegans SAS-1 ensures centriole integrity and ciliary function, and operates with SSNA-1.

53. Woglar, A. *et al.* Molecular architecture of the C. elegans centriole. *PLOS Biol.* 20, e3001784 (2022).

54. Dammermann, A. & Merdes, A. Assembly of centrosomal proteins and microtubule organization depends on PCM-1. *J. Cell Biol.* 159, 255–266 (2002).

55. Jones, L. A. *et al.* Dynein light intermediate chains maintain spindle bipolarity by functioning in centriole cohesion. *J. Cell Biol.* 207, 499–516 (2014).

56. Chen, F. *et al.* Self-assembly of pericentriolar material in interphase cells lacking centrioles. *eLife* 11, e77892 (2022).

57. Höing, S. *et al.* Dynarrestin, a Novel Inhibitor of Cytoplasmic Dynein. *Cell Chem. Biol.* 25, 357-369.e6 (2018).

58. Young, A., Dictenberg, J. B., Purohit, A., Tuft, R. & Doxsey, S. J. Cytoplasmic Dynein-mediated Assembly of Pericentrin and γ Tubulin onto Centrosomes. *Mol. Biol. Cell* 11, 2047–2056 (2000).

59. Firestone, A. J. *et al.* Small-molecule inhibitors of the AAA+ ATPase motor cytoplasmic dynein. *Nature* 484, 125–129 (2012).

60. Erpf, A. C. *et al.* PCMD-1 Organizes Centrosome Matrix Assembly in *C. elegans*. *Curr. Biol.* 29, 1324-1336.e6 (2019).

61. Shah, P. K. *et al.* An In Toto Approach to Dissecting Cellular Interactions in Complex Tissues. *Dev. Cell* 43, 530-540.e4 (2017).

62. Li, W. *et al.* Centriole translocation and degeneration during ciliogenesis in *Caenorhabditis elegans* neurons. *EMBO J.* 36, 2553–2566 (2017).

63. Banterle, N. & Gönczy, P. Centriole Biogenesis: From Identifying the Characters to Understanding the Plot. *Annu. Rev. Cell Dev. Biol.* 33, 23–49 (2017).

64. Gönczy, P. Towards a molecular architecture of centriole assembly. *Nat. Rev. Mol. Cell Biol.* 13, 425–435 (2012).

65. Magescas, J., Eskinazi, S., Tran, M. V. & Feldman, J. L. Centriole-less pericentriolar material serves as a microtubule organizing center at the base of C. elegans sensory cilia. *Curr. Biol.* 31, 2410-2417.e6 (2021).

66. Ching, K., Wang, J. T. & Stearns, T. Long-range migration of centrioles to the apical surface of the olfactory epithelium. *eLife* 11, e74399 (2022).

67. Shah, P. K. *et al.* PCP and SAX-3/Robo Pathways Cooperate to Regulate Convergent Extension-Based Nerve Cord Assembly in C. elegans. *Dev. Cell* 41, 195-203.e3 (2017).

68. Kamath, R. S. *et al.* Systematic functional analysis of the Caenorhabditis elegans genome using RNAi. *Nature* 421, 231–237 (2003).

69. Carvalho, A. *et al.* Acute Drug Treatment in the Early C. elegans Embryo. *PLoS ONE* 6, e24656 (2011).

70. Bao, Z. & Murray, J. I. Mounting Caenorhabditis elegans Embryos for Live Imaging of Embryogenesis. *Cold Spring Harb. Protoc.* 2011, pdb.prot065599 (2011).